Exp. Anim. 68(4), 417–428, 2019

—Original—

Analysis of amino acid profiles of blood over time and biomarkers associated with non-alcoholic steatohepatitis in STAM mice

Ayaka IIDA[1,2)], Sachi KURANUKI[1)], Ryoko YAMAMOTO[3)], Masaya UCHIDA[4)], Masanori OHTA[2)], Mayuko ICHIMURA[5)], Koichi TSUNEYAMA[5)], Takayuki MASAKI[6)], Masataka SEIKE[7)] and Tsuyoshi NAKAMURA[2)]

[1)]*School of Nutrition and Dietetics, Faculty of Health and Social Services, Kanagawa University of Human Services, 1-10-1 Heisei-cho, Yokosuka, Kanagawa 238-8522, Japan*
[2)]*Graduate School of Health and Environmental Sciences, Fukuoka Women's University, 1-1-1 Kasumigaoka, Higashi-ku, Fukuoka 813-8529, Japan*
[3)]*Department of Applied Biology and Food Sciences, Faculty of Agriculture and Life Science, Hirosaki University, 3 Bunkyo-cho, Hirosaki, Aomori 036-8560, Japan*
[4)]*Department of Creative Engineering, National Institute of Technology, Ariake College, 150 Higashi hagio-machi, Omuta, Fukuoka 836-8585, Japan*
[5)]*Department of Pathology and Laboratory Medicine, Institute of Biomedical Sciences, Tokushima University Graduate School, 3-18-15 Kuramoto-cho, Tokushima 770-8503, Japan*
[6)]*Department of Endocrinology, Metabolism, Rheumatology and Nephrology, Faculty of Medicine, Oita University, 1-1 Idaigaoka, Hasama-machi, Yufu, Oita 879-5593, Japan*
[7)]*Department of Gastroenterology, Faculty of Medicine, Oita University, 1-1 Idaigaoka, Hasama-machi, Yufu, Oita 879-5593, Japan*

Abstract: The changes in free amino acid (AA) levels in blood during the progression from non-alcoholic steatohepatitis (NASH) to hepatocellular carcinoma (HCC) are unclear. We investigated serum AA levels, along with biochemical and histological events, in a mouse model of NASH. We induced NASH in male C57BL/6J mice with a streptozotocin injection and high-fat diet after 4 weeks of age (STAM group). We chronologically (6, 8, 10, 12, and 16 weeks, n=4–12 mice/group) evaluated the progression from steatohepatitis to HCC by biochemical and histological analyses. The serum AA levels were determined using an AA analyzer. Serum aspartate aminotransferase and alanine aminotransferase levels were higher in the STAM group than in the normal group (non-NASH-induced mice). Histological analysis revealed that STAM mice had fatty liver, NASH, and fibrosis at 6, 8, and 10 weeks, respectively. Moreover, the mice exhibited fibrosis and HCC at 16 weeks. The serum branched-chain AA levels were higher in the STAM group than in the normal group, especially at 8 and 10 weeks. The Fischer ratio decreased at 16 weeks in the STAM group, with increasing aromatic AA levels. These results suggested that this model sequentially depicts the development of fatty liver, NASH, cirrhosis, HCC, and AA metabolism disorders within a short experimental period. Additionally, serum amyloid A was suggested to be a useful inflammation biomarker associated with NASH. We believe that the STAM model will be useful for studying AA metabolism and/or pharmacological effects in NASH.

Key words: amino acid metabolism disorder, diabetes, hyperlipidemia, non-alcoholic fatty liver disease, non-alcoholic steatohepatitis

(Received 1 October 2018 / Accepted 2 April 2019 / Published online in J-STAGE 1 June 2019)

Corresponding author: A. Iida. e-mail: iida.v9z@kuhs.ac.jp

Introduction

Non-alcoholic fatty liver disease (NAFLD) is a chronic liver disease that is strongly associated with obesity and disorders of carbohydrate metabolism [11, 13]. NAFLD is considered a comorbidity of the metabolic syndrome [20], and its types range from non-alcoholic fatty liver (simple steatosis) to non-alcoholic steatohepatitis (NASH) with progressive fibrosis without alcohol abuse [3, 33]. Among the different types of NAFLD, NASH sometimes progresses to liver diseases with a poor prognosis, including cirrhosis and hepatocellular carcinoma (HCC) [4].

Liver diseases, such as cirrhosis and HCC, generally decrease branched-chain amino acid (BCAA) levels in the blood. In fact, BCAA supplementation is used to improve the malnutrition status of patients with cirrhosis [9]. In contrast, a recent study reported that free amino acid levels in the blood of patients with obesity and NASH change with increasing levels of BCAA [14]. However, the changes in free amino acid levels in the blood during progression from NASH to HCC are unclear. Thus, there is a need to understand the free amino acid profiles in the blood to assess the state of patients with NAFLD.

Despite a dramatic increase in the number of patients with NAFLD/NASH [32], the pathogenesis and appropriate therapies are not completely understood [24]. Indeed, studies on the etiology or treatment of NASH have been hampered by the absence of a suitable experimental model. Animal models that replicate the histopathology of NASH in humans are needed to investigate the mechanisms, biomarkers, and treatment of disease [18]. Current animal models for NAFLD/NASH are generally classified into three categories: genetic models; nutritional models, such as those employing methionine and choline deficiency (MCD); and combination models with both genetic modifications and nutritional challenges [30]. However, these models do not sufficiently reflect the hepatic histopathology and pathophysiology of NASH in humans. They do not progress from fatty liver, liver inflammation, liver fibrosis, and cirrhosis to HCC along with glucose intolerance. Therefore, it is important to choose an appropriate animal model that conforms to the aims of the study [30].

In this study, we focused on a murine model for NASH (the STAM model) [8]. This model is believed to well represent the pathological progression of human NAFLD/NASH in mice and, in particular, the progression from NASH to fibrosis within a short experimental period [26]. NASH in this model is induced by an injection of streptozotocin (STZ), which is used frequently in diabetic models, along with a high-fat diet (HFD). We investigated the serum amino acid profiles over time from steatohepatitis to HCC in the STAM model. In addition, we performed DNA microarray analysis to explore biomarkers associated with NASH in STAM mice. We further assessed histopathological events in the liver and biochemical changes in liver function, sugar metabolism, and lipid metabolism.

Materials and Methods

Experiment 1

Animal model: Fourteen-day pregnant C57BL/6J mice were purchased from Charles River Laboratories Japan (Yokohama, Japan). NASH was induced through a single subcutaneous injection of 200 μg STZ (Sigma-Aldrich, St. Louis, MO, USA) in male mice at 2 days after birth, and the mice were fed High Fat Diet 32 (HFD32; CLEA Japan, Tokyo, Japan) *ad libitum* beginning at 4 weeks of age. This approach has been described previously for the STAM model [8]. The composition of HFD32 is shown in Table 1. The normal group consisted of male mice that did not receive an injection of STZ and were given *ad libitum* access to normal chow diet (CRF-1, Oriental Yeast Co., Ltd., Tokyo, Japan) after weaning. All mice were housed in a room at a temperature of 23 ± 2°C on a 12:12 h light-dark cycle and were given *ad libitum* access to tap water throughout the study. Body weight was measured every week from the start of feeding after weaning (4 weeks) to completion of the study (16 weeks).

We chronologically (at 6, 8, 10, 12, and 16 weeks) evaluated the progression of liver disease using biochemical and histological analyses in the STAM group, whereas the normal group was analyzed at 8 weeks. After fasting overnight, the mice were euthanized under anesthesia with an intraperitoneal injection of sodium pentobarbital to collect blood, white adipose tissue of the parorchis and retroperitoneum, and liver tissue. The number of STAM mice per group per time point in the analyses was 4–12. Initially, we planned to dissect STAM mice at 20 weeks (n=5). However, one mouse died unexpectedly of an unknown cause. Therefore, we dissected the rest of the mice at 16 weeks (n=4).

This study was approved by the experimental animal ethics committee of Fukuoka Women's University. All

Table 1. Composition of High Fat Diet 32 (%)

Milk casein	24.5
Powdered albumen	5.0
L-Cystine	0.43
Powdered beef tallow (beef tallow content of 80%)	15.88
Safflower oil (high-oleic type)	20.0
Cellulose	5.5
Maltodextrin	8.25
Lactose	6.928
Sucrose	6.75
AIN-93 vitamin mixture	1.4
AIN-93G mineral mixture	5.0
Choline hydrogen tartrate	0.36
t-Butylhydroquinone	0.002
	100.000

institutional and national guidelines for the care and use of laboratory animals were followed.

Biochemical analysis: The serum concentrations of aspartate aminotransferase (AST), alanine aminotransferase (ALT), total cholesterol (TCHO), triglyceride (TG), fasting blood sugar (FBS), albumin (ALB), total protein (TP), uric acid (UA), and blood urea nitrogen (BUN) were assayed using a FUJI DRI-CHEM 7000 (Fujifilm Corp., Tokyo, Japan).

Serum amino acids: To determine the amino acid levels in the blood, we deproteinized the serum with sulfosalicylic acid, and the supernatant was assayed with an amino acid analyzer (JLC-500/V2, JEOL Ltd., Tokyo, Japan). The Fischer ratio, the molar ratio of BCAA to aromatic amino acids (AAA), and the BCAA/tyrosine molar concentration ratio (BTR) were calculated.

Histological analysis: Small pieces of liver tissue were harvested, fixed immediately in 10% buffered formalin, and embedded in paraffin. Tissue sections were sectioned at a thickness of 6 μm and stained with hematoxylin and eosin (H&E) and azan. These samples were graded on the basis of Kleiner's criteria [17] to identify the degree of liver injury and fibrosis. Marginal fibrosis was evaluated as "+/−".

Experiment 2

Exposure design for microarray analysis: The STAM and normal groups were prepared as in Experiment 1. They were analyzed at 8 weeks (n=3). The tested mice were sacrificed, and their livers were removed. This liver sample collection was performed in a Petri dish filled with ice-cold RNAlater® solution (Sigma-Aldrich, St. Louis, MO, USA), and the samples were immediately frozen and stored at −30°C until the total RNA extraction and purification process was performed.

DNA microarray gene expression analysis: Total RNA samples were extracted from the exposed mice liver samples with an RNeasy Mini Kit (Qiagen, Hilden, Germany). The integrity of the extracted total RNA was evaluated using an Agilent 2100 Bioanalyzer (Agilent Technologies, Santa Clara, CA, USA), and quality-assured total RNA samples were then used for the DNA microarray analyses. For DNA microarray hybridization, antisense RNA (aRNA) was prepared using an Amino Allyl MessageAmp II aRNA Amplification Kit (Ambion, Austin, TX, USA), and Cy5 fluorescent dye (GE Healthcare, Little Chalfont, UK) was used to label the purified aRNA samples.

The DNA microarray that we used for this study was a mouse oligo DNA microarray, which was manufactured by Ecogenomics, Inc. (Fukuoka, Japan). This microarray contained 4000 oligo DNA probes (35-base-long, triplicated spots). Cy5-labeled aRNA samples were used for hybridization with the oligo DNA probes on the microarray, and hybridization was carried out for 16 h at 45°C in a hybridization solution (6× SSPE, 0.05% Tween-20, 20 mM EDTA, 25% formamide, 100 ng/μl salmon sperm DNA, 0.04% SDS). After the hybridization reaction, washing was performed in the following order and frequency of wash solutions: twice with 6× SSPE and 0.05% Tween-20 at 45°C, twice with 3× SSPE and 0.05% Tween-20 at room temperature, twice with 0.5× SSPE and 0.05% Tween-20 at room temperature, twice with 2× PBS and 0.1% Tween-20 at room temperature, and finally, twice with 2× PBS at room temperature. Each of the post-wash microarrays was scanned with a GenePix 4000B scanner at 5-μm resolution (Axon Instruments, Union City, CA, USA), and expression signal intensities were digitally processed using Microarray Imager (Combimatrix Corp., Mukilteo, WA, USA).

Experiment 3

Serum amyloid A (SAA) protein levels: The STAM and normal groups were prepared as in Experiment 1. They were analyzed at 8 weeks (n=3–9). Serum was stored at −30°C until assayed using a Mouse SAA ELISA kit (KMA0021, Invitrogen, Thermo Fisher Scientific, Waltham, MA, USA).

Statistical analyses

Statistical analyses, excluding that for the microarray data, were performed using JMP Pro 9 (SAS Institute

Inc., Cary, NC, USA). Data are expressed as the mean ± SEM. Data except SAA protein levels were analyzed using the Tukey-Kramer test, and SAA protein levels were analyzed using Student's *t*-test. A *P*-value <0.05 was considered statistically significant.

Statistical analysis of the microarray data was carried out as follows: the expression signals obtained from each of the 4,000 genes probes were background signal-subtracted and normalized by the median signal intensity per array. Then, statistical analysis was performed using the ArrayStat *z*-test (Imaging Research Inc., Piscataway, NJ, USA) with offset correction and $P<0.05$ (significance cutoff) to obtain an average expression ratio of the exposure group (n=3) to the control group (n=3) for each of the genes on the microarray.

Results

Body weight change

The changes in body weight from the start of feeding with HFD32 to 16 weeks of age are shown in Fig. 1. Mice in the STAM group progressively gained weight up to 12 weeks of age, but their body weight remained low compared with mice in the normal group. The body weight of mice in the STAM group began to decrease gradually beginning at 12 weeks. Based on the data provided by Charles River Laboratories Japan, Inc., the data for body weight showed typical changes expected in healthy male C57BL/6J mice (n=21) fed CRF-1.

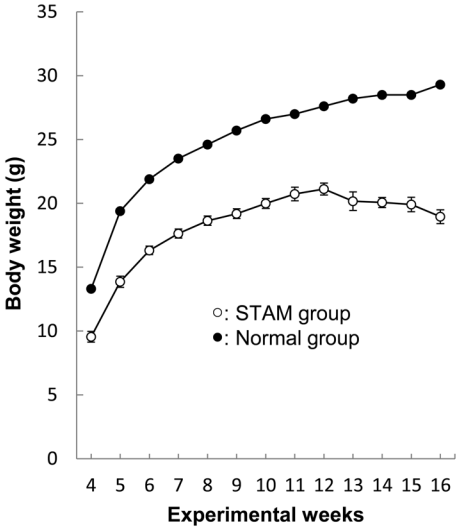

Fig. 1. Changes in the relative body weight of mice in the STAM group (at 6, 8, 10, 12, and 16 weeks, n=4–12 per group) and normal mice. Based on the data provided by Charles River Laboratories Japan, Inc., the data on body weight show typical changes expected for healthy male C57BL/6J mice (n=21) fed a normal chow diet (CRF-1).

Organ weight

The liver weight/body weight ratios of mice in the STAM group at 8 and 10 weeks were significantly higher compared with the respective values of mice in the normal group ($P<0.05$). In addition, the spleen weight/body weight ratios of mice in the STAM group at 12 and 16 weeks were significantly higher compared with the respective values of mice in the normal group ($P<0.05$). In contrast, there was no significant difference in the adipose tissue body weight ratios between mice in either group (Table 2).

Serum biochemical parameters

The activity levels of serum enzymes such as AST and ALT have been used as biochemical markers of hepatic damage. The serum AST and ALT levels were higher in mice in the STAM group than in mice in the normal group during the experimental period. The serum TCHO level was significantly higher in mice in the STAM group than in mice in the normal group ($P<0.05$). The serum TG level in the STAM group mice did not change until 12 weeks, but at 16 weeks the level was significantly higher in mice in the STAM group than in those in the normal group. FBS was significantly higher in mice in the STAM group than in those in the normal group during the experimental period. The serum ALB (all time points) and TP levels (at 8, 10, and 12 weeks) were significantly lower in the STAM group mice than in the normal group mice. There were no significant differences in the BUN and UA levels between groups, but the BUN levels tended to be higher in mice in the STAM group than in those in the normal group over time (Table 3).

Change in serum-free amino acid levels

The serum BCAA level tended to be higher in mice in the STAM group than in those in the normal group, especially at 8 and 10 weeks (Table 4). In particular, the serum isoleucine level was significantly higher in the STAM group mice at 8 weeks than in mice in the normal group. In addition, the serum BCAA levels in the mice in STAM group decreased gradually over time after 12 weeks. The serum AAA level was significant higher in the STAM group mice at 16 weeks than in mice in the

Table 2. Comparison of liver, spleen, and fat weights between normal and STAM group mice

	Normal	STAM			
	8 weeks	6 weeks	8 weeks	10 weeks	12 weeks	16 weeks
Number of mice	10	7	12	7	7	4
BW (g)	23.2 ± 0.6^{a}	13.5 ± 0.6^{b}	16.2 ± 0.6^{c}	$17.4 \pm 0.6^{c,d}$	18.9 ± 0.4^{d}	$17.6 \pm 0.3^{c,d}$
Liver weight (% BW)	6.5 ± 0.4^{a}	$7.8 \pm 0.4^{a,b}$	9.5 ± 0.4^{c}	$8.8 \pm 0.3^{b,c}$	$7.6 \pm 0.4^{a,b}$	$8.2 \pm 0.5^{a,b,c}$
Spleen weight (% BW)	0.4 ± 0.1^{a}	$0.8 \pm 0.1^{a,b}$	$0.9 \pm 0.1^{a,b}$	$1.0 \pm 0.2^{a,b}$	1.3 ± 0.3^{b}	1.4 ± 0.1^{b}
Fat[1] weight (% BW)	3.1 ± 0.3	1.7 ± 0.2	2.2 ± 0.3	2.6 ± 0.4	2.3 ± 0.5	1.7 ± 0.4

Values are expressed as the mean ± SEM. a, b, c, d: Different superscript letters indicate significant differences ($P<0.05$). [1]Epididymal and retroperitoneal white adipose tissue. BW, body weight.

Table 3. Comparison of serum levels of aspartate aminotransferase, alanine aminotransferase, total cholesterol, triglyceride, fasting blood sugar, albumin, total protein, uric acid, and blood urea nitrogen in normal and STAM mice

	Normal	STAM			
	8 weeks	6 weeks	8 weeks	10 weeks	12 weeks	16 weeks
Number of mice	10	7	11	7	7	4
AST (U/l)	61 ± 3^{a}	136 ± 16^{b}	132 ± 15^{b}	$100 \pm 9^{a,b}$	124 ± 11^{b}	133 ± 10^{b}
ALT (U/l)	24 ± 1^{a}	45 ± 5^{b}	55 ± 7^{b}	46 ± 5^{b}	$42 \pm 2^{a,b}$	$42 \pm 5^{a,b}$
TCHO (mg/dl)	77 ± 4^{a}	130 ± 6^{b}	129 ± 10^{b}	125 ± 14^{b}	124 ± 6^{b}	147 ± 17^{b}
TG (mg/dl)	117 ± 7^{a}	72 ± 10^{a}	104 ± 16^{a}	122 ± 12^{a}	115 ± 13^{a}	249 ± 68^{b}
FBS (mg/dl)	105 ± 3^{a}	529 ± 83^{b}	$583 \pm 20^{b,c}$	$647 \pm 65^{b,c,d}$	760 ± 29^{d}	$758 \pm 57^{c,d}$
ALB (g/dl)	2.4 ± 0.0^{a}	1.9 ± 0.0^{b}	1.9 ± 0.1^{b}	1.7 ± 0.1^{b}	1.7 ± 0.1^{b}	1.7 ± 0.1^{b}
TP (g/dl)	$4.6 \pm 0.1^{a,b}$	$4.1 \pm 0.0^{b,c}$	3.6 ± 0.1^{d}	$3.6 \pm 0.2^{c,d}$	$4.0 \pm 0.1^{c,d}$	$4.0 \pm 0.1^{b,c,d}$
UA (mg/dl)	1.9 ± 0.2	-	2.2 ± 0.3	-	-	2.2 ± 0.2
BUN (mg/dl)	34.1 ± 1.9	-	43.4 ± 5.2	-	-	52.2 ± 4.3

Values are expressed as the mean ± SEM. a, b, c, d: Different superscript letters indicate significant differences ($P<0.05$). A hyphen indicates that measurement was not performed. AST, aspartate aminotransferase; ALT, alanine aminotransferase; TCHO, total cholesterol; TG, triglyceride; FBS, fasting blood sugar; ALB, albumin; TP, total protein; UA, uric acid; BUN, blood urea nitrogen.

Table 4. Comparison of the Fischer ratio and branched-chain amino acid/tyrosine molar concentration ratio in normal and STAM mice

	Normal	STAM			
	8 weeks	8 weeks	10 weeks	12 weeks	16 weeks
Number of mice	10	12	7	7	4
BCAA	235 ± 13	296 ± 17	292 ± 25	275 ± 27	262 ± 32
Valine (nmol/l)	101 ± 6	127 ± 8	130 ± 12	122 ± 13	116 ± 14
Leucine (nmol/l)	84 ± 5	98 ± 6	97 ± 9	95 ± 9	88 ± 11
Isoleucine (nmol/l)	50 ± 3^{a}	70 ± 4^{b}	$66 \pm 4^{a,b}$	$59 \pm 5^{a,b}$	$58 \pm 7^{a,b}$
AAA	69 ± 4^{a}	77 ± 4^{a}	83 ± 8^{a}	78 ± 4^{a}	120 ± 22^{b}
Phenylalanine (nmol/l)	40 ± 1^{a}	$44 \pm 2^{a,b}$	$44 \pm 3^{a,b}$	$44 \pm 2^{a,b}$	55 ± 7^{b}
Tyrosine (nmol/l)	30 ± 2^{a}	33 ± 2^{a}	39 ± 5^{a}	33 ± 2^{a}	65 ± 16^{b}
Fischer Ratio[1]	$3.5 \pm 0.2^{a,b}$	3.8 ± 0.3^{a}	$3.7 \pm 0.4^{a,b}$	$3.6 \pm 0.3^{a,b}$	2.3 ± 0.3^{b}
BTR	$8.3 \pm 0.7^{a,b}$	9.3 ± 1.0^{a}	$8.3 \pm 1.2^{a,b}$	$8.4 \pm 0.9^{a,b}$	4.4 ± 0.7^{b}

Values are expressed as the mean ± SEM. a, b, c, d: Different superscript letters indicate significant differences ($P<0.05$). [1]Fischer ratio: the molar ratio of BCAA to AAA. BCAA, branched-chain amino acids; AAA, aromatic amino acids; BTR, BCAA/tyrosine molar concentration ratio.

normal group. The Fischer ratio and BTR in mice in the STAM group were significantly lower at 16 weeks than those at 8 weeks.

Macroscopic features of the liver and liver histological analysis

Fat deposits were observed in the livers of mice in the

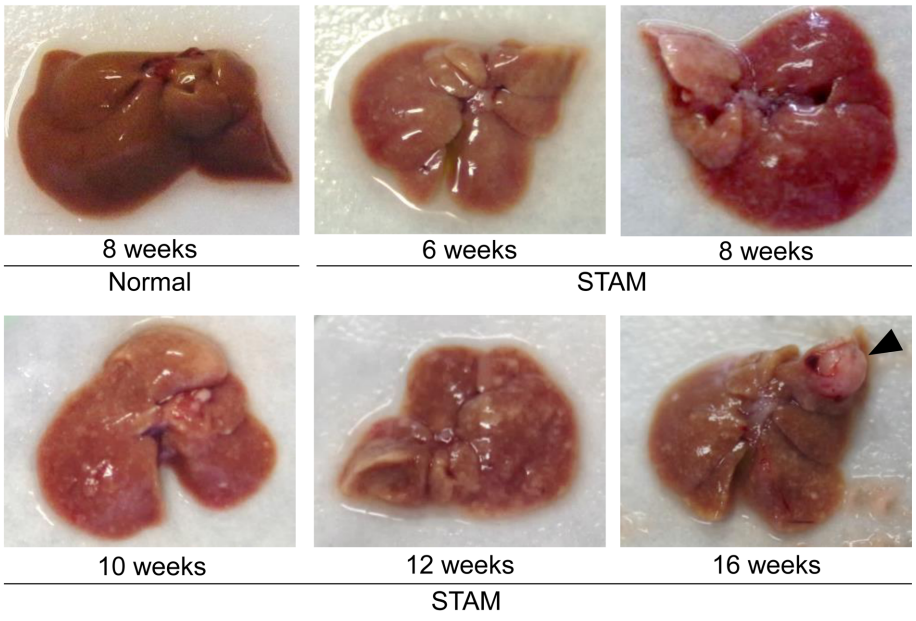

Fig. 2. Macroscopic analysis of the livers from normal and STAM group mice. Fat deposits are observed in the livers of mice in the STAM group. A macroscopic tumor-like lesion (4 × 4 mm in diameter) that was gray-white in color was detected in the liver of a mouse in the STAM group at week 16, as indicated by arrowheads.

STAM group during the experimental period. In addition, a macroscopic tumor-like lesion (4 × 4 mm in diameter) that was gray-white in color was recognized in one mouse in the STAM group at 16 weeks (Fig. 2).

A liver section with fat deposition, inflammatory cell infiltrate, fibrosis, and mild ballooning is shown in Fig. 3, and its characteristics are shown in Table 5. Progression of hepatic fibrosis was observed in mice in the STAM group at 10 and 16 weeks (Fig. 4, Table 5). The macroscopic tumor-like lesion that was observed on histological analysis in the STAM group at 16 weeks was an atypical hepatocellular nodule mimicking the early stage of human HCC (data not shown). These changes were not observed in the normal group (data not shown).

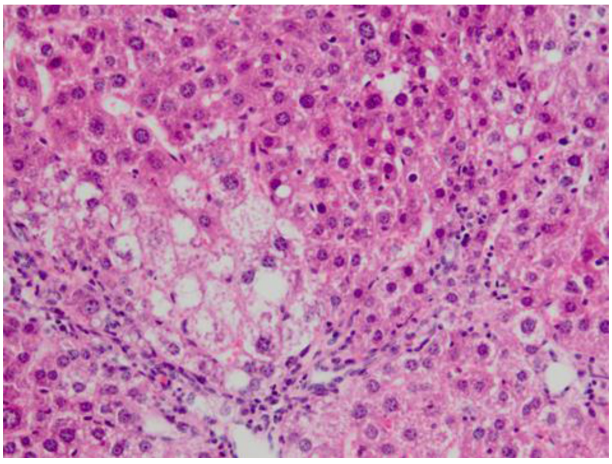

Fig. 3. Microscopic analysis of mice in the STAM group. A representative photomicrograph of a liver from a mouse in the STAM group at week 8 (H&E stain, original magnification ×200).

Gene expression analysis

We observed significant (P<0.05) expression changes (expression ratio of exposed to control >2 or <0.5) in 46 genes (14 genes were upregulated and 32 genes were downregulated) in the STAM group. Among them, 24 metabolic-related genes, 4 inflammation-related genes, 12 cancer-related genes, 4 cell cycle-related genes, and 24 toxicity-related genes were found (Table 6). In the STAM group, expression levels of serum amyloid A1 (SAA1) and serum amyloid A2 (SAA2), which are inflammation-related genes, were increased 15.06 ± 0.11-fold and 2.59 ± 0.10-fold, respectively.

SAA protein levels

The SAA level at 8 weeks was significantly higher in the STAM group mice than in the normal group mice (Fig. 5).

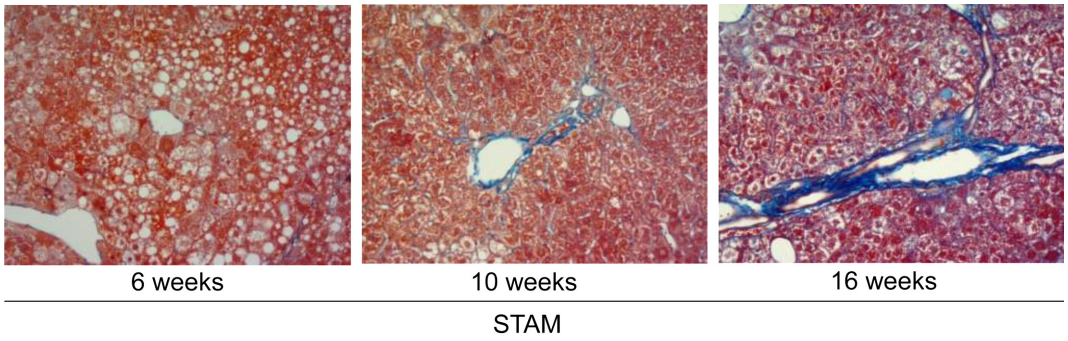

Fig. 4. Microscopic analysis of mice in the STAM group. Representative photomicrographs of the livers from mice in the STAM group at 6, 10, and 16 weeks (azan stain, original magnification ×200).

Table 5. Histopathological findings in livers of STAM mice

	STAM 6 weeks							STAM 8 weeks											
Animal no.	1	2	3	4	5	6	7	1	2	3	4	5	6	7	8	9	10	11	12
Steatosis	−	+	+	+	++	+	+	−	−	+	−	+	+	+	−	−	+	+	+
Lobular inflammation	−	−	+	+	+	+	−	−	−	+	−	−	+	−	−	−	+	+	+
Hepatocyte ballooning	+	+	+	+	+	+	+	+	+	+	+	+	+	+	+	+	+	+	+
Fibrosis	−	−	−	−	−	+	−	+/−	+/−	−	−	−	+/−	+/−	+/−	−	+/−	+/−	−

	STAM 10 weeks							STAM 12 weeks							STAM 16 weeks			
Animal no.	1[a)b)]	2	3	4	5	6	7	1[b)]	2	3[b)]	4	5	6	7	1	2[b)]	3	4
Steatosis	+	+	+	+	+	+	+	−	−	−	+	+	++	−	+	+	+	+
Lobular inflammation	+	+	+	+	−	−	−	−	+	−	−	+	−	−	+	+	+	−
Hepatocyte ballooning	+	+	+	+	−	+	+	+	+	+	−	+	+	+	+	−	+	+
Fibrosis	+	+	+	+	+/−	+	+	−	−	−	+	++	++	−	−	+	+	+

The degree of liver injury and fibrosis was graded on the basis of Kleiner's criteria [17]. Fibrosis was evaluated using H&E or azan staining. [a)]Extramedullary hematopoiesis. [b)]Hepatocellular nodule.

Table 6. Numbers of hepatic genes upregulated (>2) and downregulated (<0.5) in the STAM group at 8 weeks

Genes (4,001)	STAM
Metabolic (1,151)	
Upregulated	5
Downregulated	19
Inflammation (763)	
Upregulated	2
Downregulated	2
Cancer (993)	
Upregulated	3
Downregulated	9
Cell cycle (961)	
Upregulated	3
Downregulated	1
Toxicity (1,349)	
Upregulated	8
Downregulated	16
Total (4,001)	
Upregulated	14
Downregulated	32

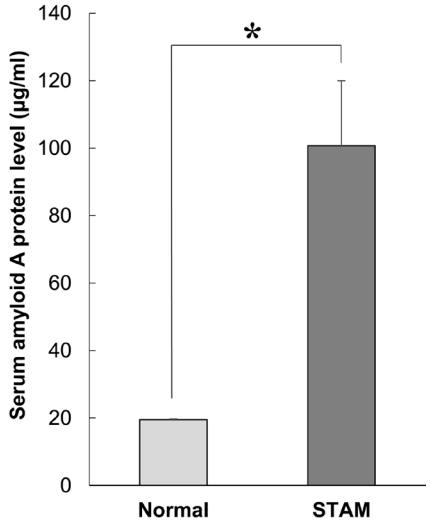

Fig. 5. Serum amyloid A protein levels in the STAM mice (n=9) and normal mice at 8 weeks (n=3). Values are expressed as the mean ± SEM. **P*<0.05.

Discussion

In this study, we clarified the changes in free amino acid levels in blood over time during the progression from NASH to HCC in mice (the STAM model, induced by an STZ injection and HFD feeding). This model is similar to the NAFLD/NASH model in humans based on the progression of histopathological events as well as biochemical and pathological characteristics.

Pathophysiological changes in hepatic lesions in STAM mice have been previously reported [27]. However, these changes have been evaluated only between 5 and 10 weeks; no study has reported the changes in the amino acid profiles of blood over time. Thus, we investigated the serum amino acid levels, along with biochemical and histological events, in STAM mice for a comparatively longer period of 16 weeks. However, the biochemical and histological events in the normal group were analyzed at 8 weeks, because at 12 weeks, these data remained almost unchanged compared with those at 8 weeks (data not shown). Additionally, it has been reported that in C57BL/6J mice fed CRF-1, serum data such as blood glucose, TG, TCHO, and ALT are almost the same between 5 and 10 weeks [27].

Presently, the "multiple parallel hits hypothesis" proposed by Tilg *et al.* [31] is well accepted for describing the pathogenesis of NAFLD/NASH. According to this hypothesis, many "hits," such as endoplasmic reticulum stress, release of (adipo) cytokines from the gut and/or the adipose tissue, and dietary factors, occur in parallel rather than consecutively and induce NAFLD/NASH. In this study, we speculated that diabetes, hyperlipidemia, and oxidative stress together play a role in the pathogenesis of NASH in the mouse model. STZ is often injected into mice to generate experimental animal models of diabetes, as it induces high blood sugar levels [10]. The diabetogenic property of STZ is characterized by the selective destruction of pancreatic β-cells, followed by hyperglycemia, which is associated with chronic inflammation [10]. In this study, we injected the mice with a low dose of STZ and subsequently fed them an HFD to induce diabetes and hypercholesterolemia during the experiment (Table 3). Plasma insulin levels were not measured in this study. However, the STAM model is reported to show impairment in insulin secretion under hyperglycemic conditions [26]. Therefore, the STAM model mice in our study might have developed type 1 diabetes mellitus, which is characterized by insulin deficiency. The body weight of mice in the STAM group remained low compared with that of mice in the normal group (Fig. 1); therefore, we presumed that severe diabetes limits growth. In addition, a continuous HFD stimulates oxidative stress [21]. Long-term exposure to an HFD for 50 weeks was previously reported to induce NAFLD/NASH in mice [12], but it is impractical to use this approach for conducting basic research on NAFLD/NASH. Additionally, among the currently available animal models for NASH, the MCD model has been widely used, although mice in this model show significant weight loss and low FBS levels [18, 30]. Recently, the Tsumura Suzuki Obese Diabetes (TSOD) mice were established as an animal model for NASH with type 2 diabetes [23]. However, this model is not suitable for investigating pharmacological effects using *in vivo* screening because of the slow course of disease from fatty liver and NASH to liver fibrosis. Therefore, use of the STAM model seemed the most appropriate to reproduce the disease status within a relatively short experimental period through a combination of STZ and HFD.

Patients with cirrhosis generally lose weight owing to poor nutrition. The mice in our model gradually lost weight after 12 weeks, and the serum ALB and TP levels remained low during the experiment (Fig. 1, Table 3). The loss of weight was believed to be caused by the poor nutritional status that was associated with severe liver disease. Among the amino acids, BCAAs are used as an alternative energy source in cases of severe liver disease, such as liver cirrhosis [15]. In fact, an amino acid imbalance is often observed in patients with cirrhosis. The Fischer ratio and BTR, which is an indicator of nutritional status calculated as the ratio of BCAA to AAA, gradually decreased with an increase in tyrosine levels in patients with severe liver disease [15]. In addition, BCAA levels were reported to decrease in patients with NASH as the liver fibrosis stage progressed, whereas tyrosine levels increased with increasing fibrotic stage [16]. In the present study, AAA levels also increased as the liver disease progressed and became severe, especially at 16 weeks (Table 4). Furthermore, the Fischer ratio and BTR tended to decrease at 16 weeks (Table 4), similar to previous findings.

Previously, BCAA levels have been shown to increase in patients with obesity and NASH because of an unknown cause [14]. The way in which free amino acid profiles in blood change over time during progression from NASH to HCC is unclear. In this study, we ob-

served that the serum BCAA levels tended to increase when mice in the STAM group developed NASH. According to a study [25], although plasma BCAA concentrations increased in C57BL/6 mice fed an HFD and a control diet, the change in plasma BCAA concentrations did not differ. In contrast, mice receiving a single intraperitoneal dose of STZ, which induces type 1 diabetes, show significantly increased plasma BCAA levels [25]. Accordingly, we speculated that diabetes is associated with an increase in serum BCAA concentrations. It is widely known that BCAAs (i.e., leucine, isoleucine, and valine) are essential amino acids, substrates for protein synthesis, and sources of energy. Additionally, leucine, isoleucine, and valine regulate many key signaling pathways [35]. For example, leucine contributes to protein synthesis. Recent studies have reported that leucine and isoleucine act as nutrient regulators, which improve glucose tolerance [5, 6, 36]. Leucine and isoleucine can stimulate insulin-independent glucose uptake in skeletal muscles *in vivo* and *in vitro*, and the effect of isoleucine is greater than that of leucine [5, 6]. In our study, BCAA levels tended to increase during the early stages, with a larger increase in isoleucine (Table 4). We speculated that the significant increase in serum BCAA isoleucine levels occurred because of improved glucose tolerance. In the STAM group, FBS tended to be lower at 8 weeks, whereas the isoleucine level was highest at this time point (Tables 3 and 4). However, based on these data, it is difficult to conclude that increasing isoleucine levels affect improvement of glucose tolerance, because the serum FBS levels were too high in STAM mice. A few studies have reported that the rise in BCAA levels in the blood contributes to insulin resistance [19, 35]. It is still unclear whether BCAA causes insulin resistance [19, 35], and the relationship among BCAA, obesity, and/or NASH deserves further exploration.

Importantly, the STAM model mimicked histopathological events, from the development of fatty liver to HCC, through a fibrosis-based pathological process. These findings are corroborated by the results of microscopic analysis. NASH is defined by the presence of hepatic steatosis and inflammation with liver cell injury (ballooning degeneration) [3, 33]. We reproduced the hepatic characteristics of NASH: steatosis, inflammation, fibrosis, and mild ballooning degeneration with predominant elevation of serum AST and ALT levels, as well as an enlarged liver at 8 weeks (Fig. 3, Tables 2, 3, and 5). Additionally, we observed that in mice in the STAM group, hepatic fibrosis gradually progressed from the start of feeding of the HFD to the end of the experiment (Fig. 4, Table 5). Presently, NASH is considered a critical risk factor for liver cirrhosis and HCC [1]. Long-standing NASH may progress to liver cirrhosis, and HCC may be an outcome [4]. At 16 weeks, mice in the STAM group developed cirrhosis, and we also observed a case of atypical hepatocellular nodules mimicking the early stage of human HCC. In addition, liver fibrosis is an important factor that contributes to portal hypertension. NASH is often reported to cause an increase in portal pressure at early stages owing to central vein occlusion, as NASH as well as alcoholic liver disease progress to hepatic fibrosis from the central vein [22]. Moreover, the spleen is believed to increase in size as the portal pressure increases in patients with liver cirrhosis [2]. Thus, the increase in spleen size observed in the mice in our study probably caused progression to liver fibrosis and portal hypertension (Table 2).

We assayed the levels of BUN to confirm the impact of hyperglycemia on the kidneys. There was no significant change at any time point (Table 3). However, hyperglycemia may have had a harmful effect on kidney function, because the concentration of BUN gradually increased. Serum TCHO was significantly higher in the STAM group mice than in the normal group mice; however, compared with serum TG in the normal group, that in the STAM group showed no significant changes between 6 and 12 weeks (Table 3). Long-term exposure to HFD32 for 70 days was reported to increase plasma TCHO levels without an increase in plasma TG, and it is presumed that excess TG accumulates in the liver [28]. HFD administration in the STAM model may induce a complex form of hyperlipidemia, because the STAM group mice in the present study developed severe hyperglycemia. Liver disease is believed to induce changes in lipoprotein synthesis and other processes, the details of which are currently unclear.

We performed a DNA microarray analysis to explore biomarkers associated with NASH in STAM mice and observed significant expression changes in 46 genes in the STAM group (Table 6). Expression levels of SAA1 and SAA2, which are inflammation-related genes, were increased in the STAM group. In addition, we assayed SAA protein levels. The SAA level at 8 weeks was significantly higher in the STAM group mice than in the normal group mice (Fig. 5). It is reported that providing an HFD or an HFD with cholesterol (HFC) induces an

increase in the expression levels of SAA in the liver [29, 34]. However, expression levels of SAA in hyperlipidemic (low-density lipoprotein receptor-deficient) HFC-fed mice, which develop NASH, increase much more than those in wild-type HFC-fed C57BL/6J mice [34]. In this study, expression levels of SAA1 and SAA protein levels markedly increased about 15- and 5-fold, respectively, in the STAM mice. Therefore, we speculated that liver inflammation rather than an HFD has a great impact on the gene expression and protein levels of SAA. SAA is an acute phase protein that is produced predominantly by the liver and increases in response to inflammatory cytokines. Moreover, it exhibits significant immunological activity by inducing the synthesis of several cytokines, by being chemotactic for neutrophils and mast cells, and by activating the inflammasome cascade, which has a key role in immune activation [7]. Thus, SAA is targeted for the treatment of diseases associated with chronic inflammation [7]. The level of C-reactive protein (CRP), which can be measured in humans, increases when there is inflammation in the body. However, we cannot measure CRP in mice. Accordingly, SAA was considered a useful biomarker for evaluating inflammation in STAM mice with NASH.

We demonstrated the first evidence for changes in the blood profiles of free amino acids during progression from NASH to HCC in a mouse model. The STAM model sequentially depicted fatty liver, NASH, fibrosis, and HCC under diabetic conditions similar to those present in human NAFLD/NASH. This model has significant advantages because it effectively induces severe liver damage, progressive fibrosis, glucose intolerance, hyperlipidemia, and amino acid metabolism disorders. The model is more efficient and reproducible than other available models, such as genetic or specific nutrition models, and shows an evident progression of liver disease in a relatively short period. Additionally, SAA was considered useful as an inflammatory marker in this model. We expect that this model will be useful for elucidating the pathogenesis of NAFLD/NASH, as well as in establishing effective treatment and prevention strategies, including nutritional therapies.

Acknowledgments

This study was supported by a JSPS Grant-in-Aid for Scientific Research (grant number 23500969 and 26350158 to T.N.).

References

1. Ascha, M.S., Hanouneh, I.A., Lopez, R., Tamimi, T.A., Feldstein, A.F. and Zein, N.N. 2010. The incidence and risk factors of hepatocellular carcinoma in patients with nonalcoholic steatohepatitis. *Hepatology* 51: 1972–1978. [Medline] [CrossRef]
2. Bolognesi, M., Merkel, C., Sacerdoti, D., Nava, V. and Gatta, A. 2002. Role of spleen enlargement in cirrhosis with portal hypertension. *Dig. Liver Dis.* 34: 144–150. [Medline] [CrossRef]
3. Chalasani, N., Younossi, Z., Lavine, J.E., Diehl, A.M., Brunt, E.M., Cusi, K., Charlton, M. and Sanyal, A.J. 2012. The diagnosis and management of non-alcoholic fatty liver disease: practice Guideline by the American Association for the Study of Liver Diseases, American College of Gastroenterology, and the American Gastroenterological Association. *Hepatology* 55: 2005–2023. [Medline] [CrossRef]
4. Cohen, J.C., Horton, J.D. and Hobbs, H.H. 2011. Human fatty liver disease: old questions and new insights. *Science* 332: 1519–1523. [Medline] [CrossRef]
5. Doi, M., Yamaoka, I., Nakayama, M., Mochizuki, S., Sugahara, K. and Yoshizawa, F. 2005. Isoleucine, a blood glucose-lowering amino acid, increases glucose uptake in rat skeletal muscle in the absence of increases in AMP-activated protein kinase activity. *J. Nutr.* 135: 2103–2108. [Medline] [CrossRef]
6. Doi, M., Yamaoka, I., Nakayama, M., Sugahara, K. and Yoshizawa, F. 2007. Hypoglycemic effect of isoleucine involves increased muscle glucose uptake and whole body glucose oxidation and decreased hepatic gluconeogenesis. *Am. J. Physiol. Endocrinol. Metab.* 292: E1683–E1693. [Medline] [CrossRef]
7. Eklund, K.K., Niemi, K. and Kovanen, P.T. 2012. Immune functions of serum amyloid A. *Crit. Rev. Immunol.* 32: 335–348. [Medline] [CrossRef]
8. Fujii, M., Shibazaki, Y., Wakamatsu, K., Honda, Y., Kawauchi, Y., Suzuki, K., Arumugam, S., Watanabe, K., Ichida, T., Asakura, H. and Yoneyama, H. 2013. A murine model for non-alcoholic steatohepatitis showing evidence of association between diabetes and hepatocellular carcinoma. *Med. Mol. Morphol.* 46: 141–152. [Medline] [CrossRef]
9. Fukui, H., Saito, H., Ueno, Y., Uto, H., Obara, K., Sakaida, I., Shibuya, A., Seike, M., Nagoshi, S., Segawa, M., Tsubouchi, H., Moriwaki, H., Kato, A., Hashimoto, E., Michitaka, K., Murawaki, T., Sugano, K., Watanabe, M. and Shimosegawa, T. 2016. Evidence-based clinical practice guidelines for liver cirrhosis 2015. *J. Gastroenterol.* 51: 629–650. [Medline] [CrossRef]
10. Goyal, S.N., Reddy, N.M., Patil, K.R., Nakhate, K.T., Ojha, S., Patil, C.R. and Agrawal, Y.O. 2016. Challenges and issues with streptozotocin-induced diabetes - A clinically relevant animal model to understand the diabetes pathogenesis and evaluate therapeutics. *Chem. Biol. Interact.* 244: 49–63. [Medline] [CrossRef]
11. Hamaguchi, M., Kojima, T., Takeda, N., Nakagawa, T., Taniguchi, H., Fujii, K., Omatsu, T., Nakajima, T., Sarui, H., Shimazaki, M., Kato, T., Okuda, J. and Ida, K. 2005. The

metabolic syndrome as a predictor of nonalcoholic fatty liver disease. *Ann. Intern. Med.* 143: 722–728. [Medline] [CrossRef]
12. Ito, M., Suzuki, J., Tsujioka, S., Sasaki, M., Gomori, A., Shirakura, T., Hirose, H., Ito, M., Ishihara, A., Iwaasa, H. and Kanatani, A. 2007. Longitudinal analysis of murine steatohepatitis model induced by chronic exposure to high-fat diet. *Hepatol. Res.* 37: 50–57. [Medline] [CrossRef]
13. Jimba, S., Nakagami, T., Takahashi, M., Wakamatsu, T., Hirota, Y., Iwamoto, Y. and Wasada, T. 2005. Prevalence of non-alcoholic fatty liver disease and its association with impaired glucose metabolism in Japanese adults. *Diabet. Med.* 22: 1141–1145. [Medline] [CrossRef]
14. Kakazu, E., Kondo, Y., Ninomiya, M., Kimura, O., Nagasaki, F., Ueno, Y. and Shimosegawa, T. 2013. The influence of pioglitazone on the plasma amino acid profile in patients with nonalcoholic steatohepatitis (NASH). *Hepatol. Int.* 7: 577–585. [Medline] [CrossRef]
15. Kato, A., and Suzuki, K. 2004. How to select BCAA preparations. *Hepatol. Res.* 30S: 30–35. [Medline] [CrossRef]
16. Kawanaka, M., Nishino, K., Oka, T., Urata, N., Nakamura, J., Suehiro, M., Kawamoto, H., Chiba, Y. and Yamada, G. 2015. Tyrosine levels are associated with insulin resistance in patients with nonalcoholic fatty liver disease. *Hepat. Med.* 7: 29–35. [Medline] [CrossRef]
17. Kleiner, D.E., Brunt, E.M., Van Natta, M., Behling, C., Contos, M.J., Cummings, O.W., Ferrell, L.D., Liu, Y.C., Torbenson, M.S., Unalp-Arida, A., Yeh, M., McCullough, A.J., Sanyal, A.J., Nonalcoholic Steatohepatitis Clinical Research Network 2005. Design and validation of a histological scoring system for nonalcoholic fatty liver disease. *Hepatology* 41: 1313–1321. [Medline] [CrossRef]
18. Larter, C.Z., and Yeh, M.M. 2008. Animal models of NASH: getting both pathology and metabolic context right. *J. Gastroenterol. Hepatol.* 23: 1635–1648. [Medline] [CrossRef]
19. Lynch, C.J., and Adams, S.H. 2014. Branched-chain amino acids in metabolic signalling and insulin resistance. *Nat. Rev. Endocrinol.* 10: 723–736. [Medline] [CrossRef]
20. Marchesini, G., Brizi, M., Bianchi, G., Tomassetti, S., Bugianesi, E., Lenzi, M., McCullough, A.J., Natale, S., Forlani, G. and Melchionda, N. 2001. Nonalcoholic fatty liver disease: a feature of the metabolic syndrome. *Diabetes* 50: 1844–1850. [Medline] [CrossRef]
21. Matsuzawa-Nagata, N., Takamura, T., Ando, H., Nakamura, S., Kurita, S., Misu, H., Ota, T., Yokoyama, M., Honda, M., Miyamoto, K. and Kaneko, S. 2008. Increased oxidative stress precedes the onset of high-fat diet-induced insulin resistance and obesity. *Metabolism* 57: 1071–1077. [Medline] [CrossRef]
22. Nakamura, S., Konishi, H., Kishino, M., Yatsuji, S., Tokushige, K., Hashimoto, E. and Shiratori, K. 2008. Prevalence of esophagogastric varices in patients with non-alcoholic steatohepatitis. *Hepatol. Res.* 38: 572–579. [Medline] [CrossRef]
23. Nishida, T., Tsuneyama, K., Fujimoto, M., Nomoto, K., Hayashi, S., Miwa, S., Nakajima, T., Nakanishi, Y., Sasaki, Y., Suzuki, W., Iizuka, S., Nagata, M., Shimada, T., Aburada, M., Shimada, Y. and Imura, J. 2013. Spontaneous onset of nonalcoholic steatohepatitis and hepatocellular carcinoma in a mouse model of metabolic syndrome. *Lab. Invest.* 93: 230–241. [Medline] [CrossRef]
24. Nugent, C., and Younossi, Z.M. 2007. Evaluation and management of obesity-related nonalcoholic fatty liver disease. *Nat. Clin. Pract. Gastroenterol. Hepatol.* 4: 432–441. [Medline] [CrossRef]
25. Sailer, M., Dahlhoff, C., Giesbertz, P., Eidens, M.K., de Wit, N., Rubio-Aliaga, I., Boekschoten, M.V., Müller, M. and Daniel, H. 2013. Increased plasma citrulline in mice marks diet-induced obesity and may predict the development of the metabolic syndrome. *PLoS One* 8: e63950. [Medline] [CrossRef]
26. Saito, K., Uebanso, T., Maekawa, K., Ishikawa, M., Taguchi, R., Nammo, T., Nishimaki-Mogami, T., Udagawa, H., Fujii, M., Shibazaki, Y., Yoneyama, H., Yasuda, K. and Saito, Y. 2015. Characterization of hepatic lipid profiles in a mouse model with nonalcoholic steatohepatitis and subsequent fibrosis. *Sci. Rep.* 5: 12466. [Medline] [CrossRef]
27. Saito, T., Muramatsu, M., Ishii, Y., Saigo, Y., Konuma, T., Toriniwa, Y., Miyajima, K. and Ohta, T. 2017. Pathophysiological analysis of the progression of hepatic lesions in STAM mice. *Physiol. Res.* 66: 791–799. [Medline]
28. Shimamura, Y., Yoda, M., Sakakibara, H., Matsunaga, K. and Masuda, S. 2013. Pu-erh tea suppresses diet-induced body fat accumulation in C57BL/6J mice by down-regulating SREBP-1c and related molecules. *Biosci. Biotechnol. Biochem.* 77: 1455–1460. [Medline] [CrossRef]
29. Stienstra, R., Mandard, S., Patsouris, D., Maass, C., Kersten, S. and Müller, M. 2007. Peroxisome proliferator-activated receptor alpha protects against obesity-induced hepatic inflammation. *Endocrinology* 148: 2753–2763. [Medline] [CrossRef]
30. Takahashi, Y., Soejima, Y. and Fukusato, T. 2012. Animal models of nonalcoholic fatty liver disease/nonalcoholic steatohepatitis. *World J. Gastroenterol.* 18: 2300–2308. [Medline] [CrossRef]
31. Tilg, H., and Moschen, A.R. 2010. Evolution of inflammation in nonalcoholic fatty liver disease: the multiple parallel hits hypothesis. *Hepatology* 52: 1836–1846. [Medline] [CrossRef]
32. Vernon, G., Baranova, A. and Younossi, Z.M. 2011. Systematic review: the epidemiology and natural history of non-alcoholic fatty liver disease and non-alcoholic steatohepatitis in adults. *Aliment. Pharmacol. Ther.* 34: 274–285. [Medline] [CrossRef]
33. Watanabe, S., Hashimoto, E., Ikejima, K., Uto, H., Ono, M., Sumida, Y., Seike, M., Takei, Y., Takehara, T., Tokushige, K., Nakajima, A., Yoneda, M., Saibara, T., Shiota, G., Sakaida, I., Nakamuta, M., Mizuta, T., Tsubouchi, H., Sugano, K. and Shimosegawa, T. 2015. Evidence-based clinical practice guidelines for nonalcoholic fatty liver disease/nonalcoholic steatohepatitis. *Hepatol. Res.* 45: 363–377. [Medline] [CrossRef]
34. Wouters, K., van Gorp, P.J., Bieghs, V., Gijbels, M.J., Duimel, H., Lütjohann, D., Kerksiek, A., van Kruchten, R., Maeda, N., Staels, B., van Bilsen, M., Shiri-Sverdlov, R. and Hofker, M.H. 2008. Dietary cholesterol, rather than liver

steatosis, leads to hepatic inflammation in hyperlipidemic mouse models of nonalcoholic steatohepatitis. *Hepatology* 48: 474–486. [Medline] [CrossRef]

35. Zhang, S., Zeng, X., Ren, M., Mao, X. and Qiao, S. 2017. Novel metabolic and physiological functions of branched chain amino acids: a review. *J. Anim. Sci. Biotechnol.* 8: 10. [Medline] [CrossRef]
36. Zhang, Y., Guo, K., LeBlanc, R.E., Loh, D., Schwartz, G.J. and Yu, Y.H. 2007. Increasing dietary leucine intake reduces diet-induced obesity and improves glucose and cholesterol metabolism in mice via multimechanisms. *Diabetes* 56: 1647–1654. [Medline] [CrossRef]